



Research paper

Different configurations of the non-minimal tensegrity triplex

Andrzej Rutkiewicz¹

Abstract: The paper presents analyses on stable prestressed configurations of the tensegrity triplex with a non-minimal number of members. The non-minimal triplex is generally understood in the literature as the minimal triplex with three additional cables. However, this research shows that many different configurations can be obtained during prestressing. The prestressing procedure is led by changing the lengths of selected groups of members, i.e., struts, horizontal cables, cross cables, or additional members, assuming symmetry. A different view on prestressing is presented, where typically understood tensegrity natural configuration is separated into a newly called geometrical configuration and natural lengths of attached members. The presented interpretation of prestressing has a clear physical meaning. The calculations are based on the elastic energy approach, which is used to write the nonlinear equations that are afterward solved numerically. Two examples of prestressing the non-minimal triplex are presented, for slender and stocky prisms dimensions. The results show that additional members usually understood in the literature as additional cables, can as well serve as struts, which leads to a new group of structures with tensegrity features.

Keywords: energy approach, non-minimal prism, prestress, prismatic tensegrities, truss

¹PhD., Eng., University of Warmia and Mazury in Olsztyn, Faculty of Geoen지니어ing, ul. Prawocheńskiego 15, 10-720 Olsztyn, Poland, e-mail: andrzej.rutkiewicz@uwm.edu.pl, ORCID: 0000-0001-8664-5093

1. Introduction

Tensegrities are a subclass of spatial trusses, which members are built from struts, which transfer only compression and cables, which transfer only tension. The load bearing capacity and stability of these trusses is dependent on the prestressing of the whole system. Tensegrities may experience large displacements, even though the strains in members may remain small, which originates from a so called infinitesimal mechanism phenomenon. More basic information and current trends can be found in [1–3], while some inspirations can be found in the works of the artist Kenneth Snelson [4].

The minimal and regular triplex, is one of the most well-known, as well as firstly invented and patented tensegrity [5–7] – see Fig. 1a for a fragment of Snelson’s patent. Term minimal refers to the fact that it possesses the least number of members required to obtain a stable configuration [8], while term regular refers to the fact, that members of the same type are of equal length [9]. The angle of rotation between the upper and lower base along the vertical axis is equal to $5\pi/6$, which is a characteristic value for stable configuration. Different types of members are presented in Fig. 1b by individual colours and are: six horizontal cables creating two parallel bases (orange), three cross cables (blue) and three struts (red). Please note that for better clarity of view only one member of each non-horizontal group is presented.

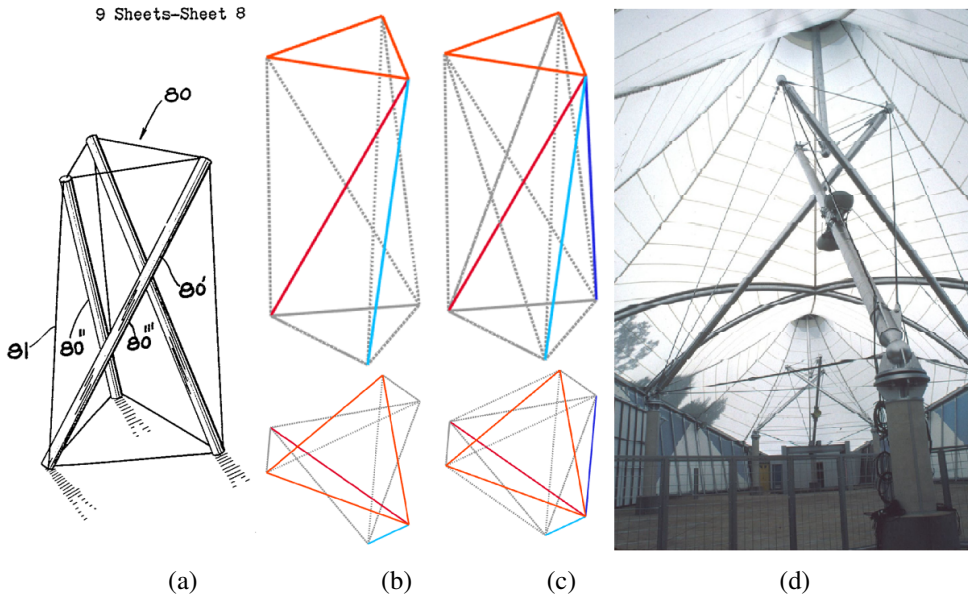


Fig. 1. The triplex: a) Snelson’s patent, b) minimal one, c) non-minimal one and d) the White Rhino I

The non-minimal triplex is the variation of the minimal one created by attaching additional members (three) – see violet line in Fig. 1c. What will be shown is that these members can be struts or cables, depending on the obtained configuration.

The minimal and regular triplex is the one that possesses the least number of elements from a so called prismatic tensegrity systems [9], as in the classification given by A. Pugh [10]. Prismatic tensegrity systems include all of the t -strut configurations such as the triplex ($t = 3$), the quartex ($t = 4$), the pentex ($t = 5$) and so on. Figure 1a,b presents the triplex. One of the first studies on these trusses was performed by [11] to be followed by [12] and others [13, 14]. Currently, these systems are intensively studied. In [15] a generalized form of prismatic tensegrities, which possess dihedral symmetry, was presented. In [16] the connectivity, incidence and node matrices for all t -strut prismatic tensegrities in an analytical form were presented. In [17] prismatic systems with additional cable nets were analysed. In the publication [18], methods of morphogenesis of icosahedral and prismatic tensegrities, which was also practically used to analyse a tensegrity footbridge, were studied. Also, other studies were performed on triplex or quartex prisms, not for general prismatic tensegrities. In [19,20] the quartex modules were printed and tested experimentally in compression. In [21] a parametric analysis on single triplex and quartex modules, as well as towers build from them were analysed for dynamic instabilities, whereas in [22] an identification of self-stress states, infinitesimal mechanisms, as well as behaviour under time-independent external loads was analysed. Double-layered tensegrity grids build from triplex and quartex modules were analysed in [23]. In [24] the influence of initial imperfections of struts was analysed for the mechanical response of the triplex modules, among other modules. In [25] the influence of prestress on the behaviour of a tensegrity spring chain build from triplex modules was analysed. A physical model of tensegrity triplex, with metal rubber insert in the struts was analysed in compression [26]. Finally, identification of modes and frequencies of a physical model of tensegrity triplex was performed in [27]. In some cases also the influence of support conditions was analysed, which is a rather rare find [28,29].

However, not much work has been done in case of prismatic tensegrities with non-minimal number of members. The most comprehensive survey on non-minimal prismatic tensegrities was performed in [30], where a group of up to seven-strut prisms were analysed. In the study, the minimal prisms were firstly prestressed, afterwards additional cables were attached and their length was shortened creating the non-minimal configurations. This procedure is called a reconfiguration following by the definition from [31]. On the other hand, the non-minimal triplex, i.e. 3-strut prism was studied briefly in [8], where force densities were determined at a range of 15-degree angle twist between the upper and lower bases. Also, a real scale realizations of this prism were erected, i.e. the White Rhinos (Fig. 1d [32] presents White Rhino I), a membrane structures in which the non-minimal triplex is serving as a support [32, 33]. Also, a structure which was said to be a support of the triangular truss bridge was reported in [34] and is clearly a non-minimal triplex. Regardless to the fact, that the non-minimal prisms were not widely analysed, the concept of attaching additional cables to prismatic systems was reported in the literature due to the fact that it eliminates the infinitesimal mechanisms causing the structure to stiffen. In [35] a quartex tensegrity tower was analysed with and without additional cables, while in [36] a whole additional cable net influence was analysed for prismatic tensegrities.

All of the previously cited work has assumed that additional members on the tensegrity triplex are cables. The novelty of this work lies in the discovery that additional cables attached to the minimal triplex, can as well become struts, depending on the angle of rotation between the upper and lower bases along the vertical axis of the system. This enables to understand the non-minimal prismatic tensegrities as not only the minimal prisms with additional cables but a whole new group of tensegrities, which can be classified as “structures with tensegrity features”.

The basis of such search lies in the will to implement tensegrities into civil engineering field. This is a difficult task, which is indicated even by the low number of erected structures. High requirements of stiffness and cost-effectiveness in the design of typical civil engineering structures causes the initial tensegrity design concepts to become more or less simple trusses than tensegrities itself. Therefore, a search of trusses lying somewhere between the lookalike tensegrities and being able to be implement in the design field is performed.

The paper is organised as follows. Chapter 2 contains the non-minimal triplex equations derived based on the energy approach, as well as basic assumptions and a new proposition to the prestressing procedure. Chapter 3 contains numerical analyses on two examples of slender and stocky non- minimal triplex prisms with discussion. Chapter 4 encloses the article with conclusions. Also, annex contains partial derivatives to the presented equations.

2. Methods

2.1. Basic assumptions

An assumption on symmetry is made, where all members of the same type possess the same initial lengths. Moreover, during prestressing the members of the same type form a group, where all members of this particular group are prestressed simultaneously, i.e. the change of length is applied to all group members. This simplifies the energy equations making them shorter and practically able to be derived. Since the number of self-stress states for the triplex is equal to three [30], the minimal number of members inducing the prestress is also three. These members are not arbitrary chosen. However, selection of prestress groups fulfils the requirements, where at least three members are a part of a group, as well each of them is a part of one localized self-stress state (for definition of localized self- stress states please refer to [37]). These groups are: six horizontal cables with length denoted as l , three struts with length denoted as b , three cross cables with length denoted as s and three additional members with length denoted as a . The consequences of the symmetry are that every possible symmetrical configuration of the non- minimal triplex can be defined by only three independent variables. Therefore, we consider the process of symmetrical transition from the unstressed state to the prestress state.

The initial angle of rotation between the upper and lower bases α needs to be established for the initial configuration. Here, the angle α is zero, when struts are vertical, as in for example [38]. Please note that in many publications this angle is calculated starting from

vertical cables (for example in [39]). Therefore the angle at initial configuration is equal to $\alpha = 5\pi/6$. Now, for every analysed prism, a new measure of angle θ is introduced, which is equal to zero at the initial configuration, i.e. for α equal to $5\pi/6$. The angle θ has its limitations during the rotation in the prestressing process. The locking of struts occurs at:

$$(2.1) \quad \theta_{\max} = \pi - \alpha = \pi/6$$

i.e. for a counterclockwise rotation. Locking of struts and additional members occurs when:

$$(2.2) \quad \theta_{\min} = 2\pi/3 - \alpha = -\pi/6$$

i.e. for a clockwise rotation. In the study, the material is linearly elastic and strains are assumed to be small.

2.2. Energy based equations

Nodes and member connections of the non-minimal triplex are presented in Fig. 2a, b, where colours of members are given analogically as in Fig. 1c.

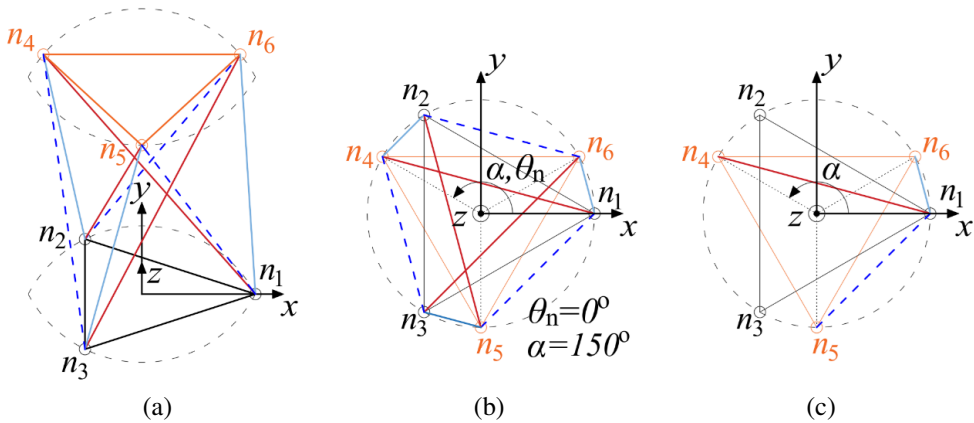


Fig. 2. The non-minimal triplex view: a) axonometry, b) top and c) connections between nodes

For a known value of twist angle $\alpha = 5\pi/6$ the node coordinates, which depend on three variables θ , b and r , can be written as:

$$(2.3) \quad \begin{aligned} n_1 & (r, 0, 0) & n_4 & (r \cos(\theta + 5\pi/6), r \sin(\theta + 5\pi/6), h) \\ n_2 & (-r/2, \sqrt{3}r/2, 0) & n_5 & (r \cos(\theta + 11\pi/6), r \sin(\theta + 11\pi/6), h) \\ n_3 & (-r/2, -\sqrt{3}r/2, 0) & n_6 & (r \cos(\theta + \pi/6), r \sin(\theta + \pi/6), h) \end{aligned}$$

where: r is the radius of the circles circumscribed on triangles created from bottom and top horizontal cables, h is the height and θ was defined before.

Please note that in the initial configuration $\theta = \theta_n = 0$, $b = b_n$ and $r = r_n$, where n -index refers to the unstressed lengths of all members, i.e. to an unstable configuration, since there is no prestressing. This direction of rotation creates a so called left-handed triplex – see [38]. Also, an assumption on which members are struts and which are cables is already made, prior to the form-finding process. Based on Fig. 2c one can write the lengths of struts, i.e. cross cables, i.e. and additional members, i.e. Please note that other nodes could be taken into consideration, yet due to symmetry it is a matter of arbitrary selection. Therefore, the height h and dependant lengths are:

$$(2.4) \quad \begin{aligned} h &= \sqrt{b^2 - r^2(2 + \sqrt{3} \cos \theta + \sin \theta)}, & s &= \sqrt{b^2 - 2\sqrt{3}r^2 \cos \theta}, \\ a &= \sqrt{b^2 - r^2(3 \sin \theta + \sqrt{3} \cos \theta)} \end{aligned}$$

Also, the relation between the radius length r and horizontal cable length is $l = r\sqrt{3}$. After prestressing, the total elastic energy U of the system is:

$$(2.5) \quad U = \frac{3}{2}k_s(s - s_n)^2 + \frac{3}{2}k_b(b - b_n)^2 + \frac{3}{2}k_a(a - a_n)^2 + 6\frac{1}{2}3k_l(r - r_n)^2$$

where: k_s , k_b , k_a and k_l are the axial stiffnesses of cross cables, struts, additional members and horizontal cables, respectively; the n -indexed lengths refer to the unstressed, while unindexed to prestressed lengths.

Finding the extremum of the energy U requires to identify and classify the critical points by comparing to zero the partial derivatives with respect to the variables θ , r and b and then to examine the Hessian matrix. The first necessary condition gives the following system:

$$(2.6) \quad \begin{cases} \partial U / \partial \theta = 0 \\ \partial U / \partial b = 0 \\ \partial U / \partial r = 0 \end{cases} \rightarrow \begin{cases} 3k_s(s_0 - s_n)\partial s / \partial \theta + 3k_a(a_0 - a_n)\partial a / \partial \theta = 0 \\ 3k_s(s_0 - s_n)\partial s / \partial b + 3k_a(a_0 - a_n)\partial a / \partial b + 3k_b(b_0 - b_n) = 0 \\ 3k_s(s_0 - s_n)\partial s / \partial r + 3k_a(a_0 - a_n)\partial a / \partial r + 18k_l(r_0 - r_n) = 0 \end{cases}$$

where the variables s and a are given in Eq. (2.4) and their first partial derivatives are given in the Annex. Critical points, local maximum and local minimum or saddle point is verified by analysing the following Hessian:

$$(2.7) \quad \mathbf{H}(\theta, b, r) = \begin{bmatrix} \partial^2 U / \partial \theta^2 & \partial^2 U / \partial \theta \partial b & \partial^2 U / \partial \theta \partial r \\ \partial^2 U / \partial b \partial \theta & \partial^2 U / \partial b^2 & \partial^2 U / \partial b \partial r \\ \partial^2 U / \partial r \partial \theta & \partial^2 U / \partial r \partial b & \partial^2 U / \partial r^2 \end{bmatrix}$$

The second derivatives of the system and energy are also gathered in the Annex. The member forces are calculated with the assumption of Hooke's law and small strains, i.e.:

$$(2.8) \quad N_s = k_s(s - s_n), \quad N_b = k_b(b - b_n), \quad N_a = k_a(a - a_n), \quad N_l = k_l(l - l_n),$$

where: $N_s, N_b, N_a, N_l \in R$ are axial forces in cross cables, struts, additional members and horizontal cables, respectively.

2.3. Prestressing process

Here, a reference to simple physical interpretation of prestressing is presented based on the minimal triplex – see Fig. 3. In general, two states of whichever tensegrity are distinguished, i.e. the geometrical state (Fig. 3a) and the prestressed state (Fig. 3c). The geometrical configuration descends from the necessity of members to connect in nodes and it is a state where theoretical lengths are considered. These lengths are g -indexed. If all natural lengths, indexed with n , understood as actual physical lengths of members, are equal to geometrical lengths, then there is no prestress and the system is unstable (Fig. 3a). For example, if natural lengths of struts and horizontal cables in Fig. 3b are equal to geometrical lengths, while cross cables natural lengths are shorter than geometrical ones, the prestressing occurs (Fig. 3c). Therefore, a clear interpretation of the cause of prestress is given, i.e. shorter cross cables are stressing other members.

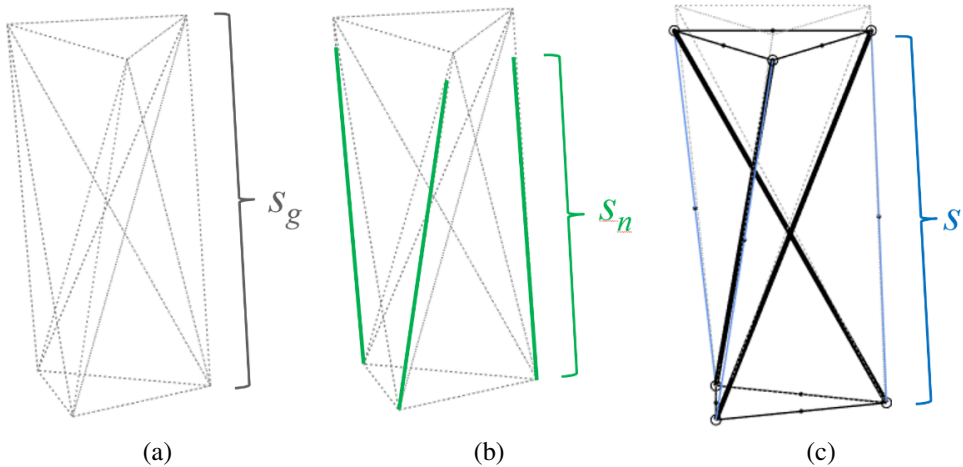


Fig. 3. Prestressing: a) geometrical state, b) attached natural lengths of members and c) prestressed state

This is a different approach, where in some publications a so called natural state is introduced (see for example [38]), where geometrical connectivity and natural lengths are considered as one. If so, there is a lack of physical interpretation on the cause of prestress between the natural state and the prestressed state, i.e. there is no length change which would cause the structure's members to prestress. In practical numerical calculations this was approached by assuming one prestressed length and afterwards recalculating others, as well as at the end the corrected natural lengths needed to be substituted. Approach presented here possesses a physical meaning and is easier to be programmed, i.e. only one solver is needed to find the prestressed lengths, no matter which group of members is causing the prestress, as well as no corrections needs to be made. The relations between the geometrical and natural lengths are:

$$(2.9) \quad s_n = c_s s_g, \quad b_n = c_b b_g, \quad a_n = c_a a_g, \quad l_n = c_l l_g$$

where: $c_s, c_b, c_a, c_l \in R^+$ are prestress coefficients in cross cables, struts, additional members and horizontal cables, respectively.

Please note that using these coefficients sets a clear relation between the geometrically feasible lengths (i.e. the distances between the nodes in the unstressed state) and the actually attached lengths of the members (i.e. unstressed lengths of members). This approach is different since at this stage one is not considering the stresses nor strains, i.e. these will occur after the attachment is performed. Setting $c_i > 1.0$ will lengthen the member, setting $c_i < 1.0$ will shorten the member and setting $c_i = 1.0$ will denote that the natural length is equal to geometrical one. Using Eq. (2.4), Eq. (2.6) and Eq. (2.9), as well as substituting the partial derivatives results in a system:

$$(2.10) \quad \begin{cases} k_s(1 - c_s s_g/s) \sin \theta - \frac{1}{2}k_a(1 - c_a a_g/a)(\sqrt{3} \cos \theta + \sin \theta) = 0 \\ k_s(1 - c_s s_g/s) + k_a(1 - c_a a_g/a) + k_b(1 - c_b b_g/b) = 0 \\ k_s(1 - c_s s_g/s) \cos \theta - \frac{1}{2}k_a(1 - c_a a_g/a)(\cos \theta - \sqrt{3} \sin \theta) - \sqrt{3}k_l(1 - c_l r_g/r) = 0 \\ s^2 = b^2 - 2\sqrt{3}r^2 \cos \theta \\ a^2 = b^2 - \sqrt{3}r^2(\sqrt{3} \sin \theta - \cos \theta) \end{cases} .$$

Please note that in Eq. (2.10) the prestress of the system is controlled only by c_i coefficients and more than one group can cause the prestress. However then, the coefficients are not freely chosen and need to be selected in proper compatibility. Equation (2.10) is solved numerically for θ , b , r , s and a using Matlab *fsolve* function with chosen *trust-region-dogleg* algorithm, while positive definition of Hessian from Eq. (2.7) is verified on specific numbers using Matlab *eig* function.

3. Numerical analyses

3.1. Example 1 – slender prism

Here, a so called slender prism is analysed, where $h_g/r_g = 3.50$. Geometrical lengths are: $r_g = 500$ mm ($l_g = 866.03$ mm) and $b_g = 2000$ mm, and the dependent lengths are: $s_g = 1770.3$ mm and $a_g = 1888.6$ mm. The structure's geometrical height is $h_g = 1751.3$ mm. The assumed product of Young's modulus and cross sectional area is $E_s A_s = E_b A_b = E_l A_l = E_a A_a = 10^3$ N resulting in stiffnesses equal to: $k_s = 0.5649$ N/mm, $k_b = 0.5$ N/mm, $k_a = 0.4750$ N/mm and $k_l = 1.1547$ N/mm. Please note that here stiffnesses are calculated based on geometrical lengths, while in numerical calculations they are referred to the natural lengths. The prism is prestressed based on five different scenarios (denoted from 'a' to 'e') such as: a) $c_s = 0.9$ (and $c_l = c_b = c_a = 1.0$), b) $c_l = 0.9$ (and $c_s = c_b = c_a = 1.0$), c) $c_a = 1.03$ (and $c_s = c_b = c_l = 1.0$), d) $c_a = 0.97$ (and $c_s = c_b = c_l = 1.0$) and e) $c_b = 1.1$ (and $c_s = c_a = c_l = 1.0$).

The results of calculated dimensions and forces are presented in Table 1. The bold lengths in the table refer to members, for which the natural length is different than the geometrical one. In other cases the natural and geometrical lengths are similar. The stable configurations are obtained for $0 < c_s, c_l < 1.0$, $c_b > 1.0$ and $c_a > 0$. The information referring from the last coefficient means that the additional member can be lengthened (for $c_a > 1.0$) or shortened (for $1.0 > c_a > 0$).

Table 1. Results on prestressed dimensions of the slender prism

| Prestressed group | a | b | c | d | e |
|---|-------------|---------------|----------------|----------------|-------------|
| c_i (-) | $c_s = 0.9$ | $c_l = 0.9$ | $c_a = 1.03$ | $c_a = 0.97$ | $c_b = 1.1$ |
| Physical dimensions of attached members | | | | | |
| r_n (mm) | 500 | 450 | 500 | 500 | 500 |
| b_n (mm) | 2000 | 2000 | 2000 | 2000 | 2200 |
| s_n (mm) | 1593.27 | 1770.30 | 1770.30 | 1770.30 | 1770.30 |
| a_n (mm) | 1888.65 | 1888.65 | 1945.31 | 1831.99 | 2105.47 |
| l_n (mm) | 866.03 | 779.42 | 866.03 | 866.03 | 866.03 |
| Prestressed dimensions and forces | | | | | |
| r (mm) | 507.04 | 451.21 | 500.34 | 500.29 | 506.77 |
| b (mm) | 1914.73 | 1976.64 | 1995.74 | 1994.88 | 2065.87 |
| θ (Deg) | -16.0 | -1.0 | -16.32 | 15.56 | 12.93 |
| s (mm) | 1676.35 | 1789.40 | 1775.02 | 1773.22 | 1844.10 |
| a (mm) | 1857.64 | 1888.21 | 1943.66 | 1833.18 | 1913.61 |
| l (mm) | 878.22 | 781.52 | 866.61 | 866.52 | 877.76 |
| h (mm) | 1671.79 | 1775.09 | 1771.02 | 1730.38 | 1806.42 |
| N_s (N) | 52.14 | 10.79 | 2.66 | 1.64 | 41.69 |
| N_b (N) | -42.63 | -11.68 | -2.13 | -2.56 | -60.97 |
| N_a (N) | -16.42 | -0.23 | -0.84 | 0.65 | 13.22 |
| N_l (N) | 14.08 | 2.69 | 0.67 | 0.57 | 13.55 |

The graphical results are presented in Fig. 4, where thick lines denote compressed members (struts) and thin lines denote tensioned members (cables). The member, which is the cause of prestress is denoted in red, if it is a strut (the member was lengthen, therefore is compressed) and in blue, if it is a cable (the member was shorten, therefore is tensioned).

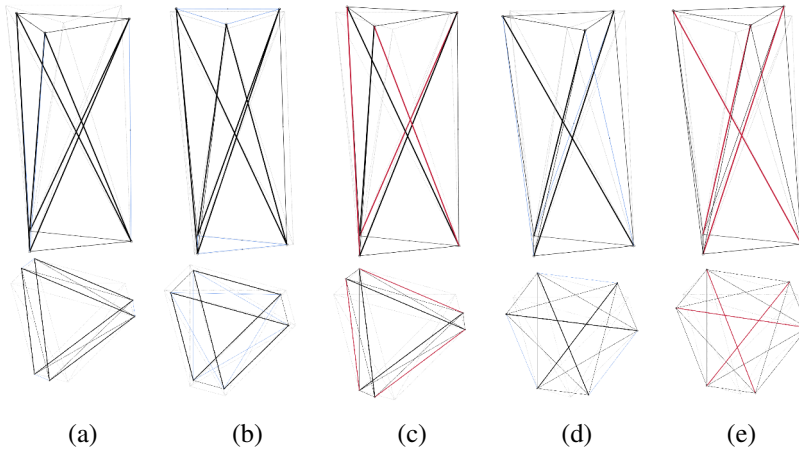


Fig. 4. Slender prism configurations prestressed by: a) cross cables, b) horizontal cables, c), d) additional members and e) struts

3.2. Example 2 – stocky prism

Another example concerns a so called stocky prism, where $h_g/r_g = 1.0$. Geometrical lengths are: $r_g = 500$ mm ($l_g = 866.03$ mm) and $b_g = 1088$ mm, and the dependent lengths are: $s_g = 563.67$ mm and $a_g = 866.45$ mm. The structure's geometrical height is $h_g = 500.73$ mm. Therefore, the radius remains the same, only the length of the strut is modified. The assumed product of Young's modulus and cross sectional area is again $E_s A_s = E_b A_b = E_l A_l = 10^3$ N and results in stiffnesses equal to: $k_s = 1.7741$ N/mm, $k_b = 0.9191$ N/mm, $k_a = 1.1541$ N/mm and $k_l = 1.1547$ N/mm. Similar set of prestressing scenarios as in case of the slender prism are chosen for the prestressing procedure. Figure 5 and Table 2 presents the results.

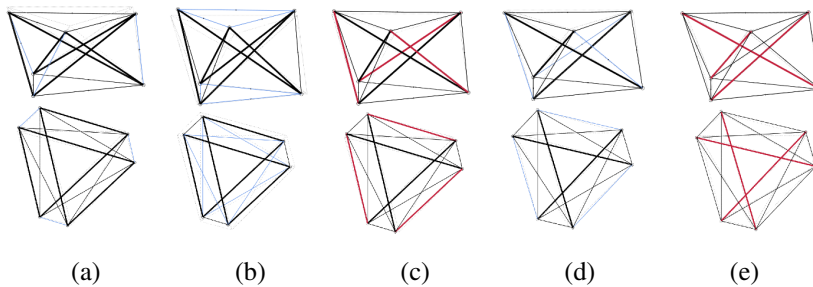


Fig. 5. Stocky prism configurations prestressed by: a) cross cables, b) horizontal cables, c), d) additional members and e) struts

Table 2. Results on prestressed dimensions of the stocky prism

| Prestressed group | a | b | c | d | e |
|---|---------------|---------------|---------------|---------------|---------------|
| c_i (-) | $c_s = 0.9$ | $c_l = 0.9$ | $c_a = 1.03$ | $c_a = 0.97$ | $c_b = 1.1$ |
| Physical dimensions of attached members | | | | | |
| r_n (mm) | 500 | 450 | 500 | 500 | 500 |
| b_n (mm) | 1088 | 1088 | 1088 | 1088 | 1196.8 |
| s_n (mm) | 507.30 | 563.67 | 563.67 | 563.67 | 563.67 |
| a_n (mm) | 866.45 | 866.45 | 892.44 | 840.45 | 866.45 |
| l_n (mm) | 866.03 | 779.42 | 866.03 | 866.03 | 866.03 |
| Prestressed dimensions and forces | | | | | |
| r (mm) | 504.39 | 460.33 | 500.11 | 500.10 | 514.41 |
| b (mm) | 1068.52 | 1034.17 | 1087.50 | 1087.53 | 1119.61 |
| θ (Deg) | -3.54 | -3.83 | -3.53 | 3.35 | 2.94 |
| s (mm) | 511.97 | 580.58 | 563.81 | 563.78 | 581.46 |
| a (mm) | 865.52 | 863.67 | 892.42 | 840.47 | 868.95 |
| l (mm) | 873.63 | 797.32 | 866.22 | 866.19 | 890.98 |
| h (mm) | 456.99 | 541.88 | 515.19 | 485.25 | 502.99 |
| N_s (N) | 9.22 | 30.01 | 0.26 | 0.21 | 31.56 |
| N_b (N) | -17.90 | -49.48 | -0.46 | -0.43 | -64.49 |
| N_a (N) | -1.08 | -3.32 | -0.03 | 0.02 | 2.88 |
| N_l (N) | 8.78 | 22.96 | 0.22 | 0.19 | 28.82 |

3.3. Discussion

Based on two presented examples, two different configurations can be obtained, i.e. for a structure with six struts is obtained (additional members work as struts), while for a structure with three struts is obtained (additional members work as cables). This is independent of the prestressing method, as long as, the rotations are in the assumed angle range, i.e. Prestressing by shortening the cross and horizontal cables generates the six strut structure (additional members are compressed, see Fig. 4a,b), while prestressing by lengthening the struts creates the three strut structure (additional members are tensioned, see Fig. 4e). Prestressing by the additional members creates the six strut structure when these members are lengthened (Fig. 4c) and the three strut structure when these members are shortened (Fig. 4d).

Also, analysing data from Table 1 shows, that small changes of lengths of additional members create large changes in θ_0 angle in regards to changes of struts, cross cables or horizontal cables. For example, setting $c_a = 1.03$ creates similar angle change as setting $c_s = 0.9$ ($\theta_0 \approx -16^\circ$). Similar observations can be made by analysis of Table 2.

What is also visible is that the slender prism has a tendency to rotate more, in regards to the stocky prism. This is visible, since similar changes of prestress coefficients create smaller rotations – again comparison between Table 1 and Table 2 results.

4. Conclusions

In the paper, a first representative of a possibly new group of “structures with tensegrity features” based on prismatic systems with non-minimal number of members was proposed. A reference to the term “structures with tensegrity features” is based on one selected criteria of classification presented in [40]. The presented prism is not a “pure tensegrity” in terms of mentioned classification, since it does not possess the infinitesimal mechanisms stiffened by the self-stress states, as well as the six strut tensegrity (Fig. 4a–c, Fig. 5a–c) is not of class one (struts interconnect with other struts). Please note however, that the “typical” nonminimal triplex (Fig. 1c,d) for angle of rotation $\theta_0 = 0$ also does not possess the infinitesimal mechanisms, therefore would be classified similarly. This representative is the prism created from the non-minimal tensegrity triplex ($t = 3$), however understood differently as in the literature up to date. Namely, there is not only one non-minimal triplex for the angle $\theta = 0$ (the one with additional cables), yet there are infinite number of non-minimal tensegrity triplexes in a angle range of What is interesting is that depending on the angle of rotation sign θ one can obtain a six struts and three cross cables configuration or three struts and six cross cables configuration. Also, prestressing using additional members is very effective in changing the value of the angle of rotation θ , where even small changes of length of the additional members increase the angle rapidly. This is expected due to the fact that the additional members are working more or less in the direction of the infinitesimal mechanism of the minimal triplex. Moreover, slender prisms tend to rotate more than stocky ones.

In addition, a physical and practical interpretation of the prestressing procedure was presented. Division of dimensions on the geometrically feasible lengths and natural lengths of the actually attached members gives a good insight into the physical process of prestress.

In general, these prisms were sought in order to find structures, which look like tensegrities, yet have a set of favourable properties usable in civil engineering. These properties are concerned mainly with stiffness and load bearing capacity. The non-minimal triplex presented here does not possess any infinitesimal mechanisms, as well as can possess six struts, which can be favourable in increasing the load bearing capacity for gravitational loads. Nevertheless, this matter is not solved yet and requires further studies.

Moreover, the energy approach was proposed to solve the issue, which is lately less used in regards to the force density method [41] and geometrically nonlinear finite element method [42].

As for the future work, it is important to verify, whether this concept can be extended to t -strut prismatic tensegrities. Moreover, a physical verification of presented numerical calculations would be valuable. Finally, analyses on mechanical response under external loading, in comparison to the minimal prisms, would be valuable.

References

- [1] R.W. Burkhardt, *A Practical Guide to Tensegrity Design*. Cambridge, MA, USA: Robert William Burkhardt, 2004.
- [2] V. Gomez-Jauregui, A. Carrillo-Rodriguez, C. Machado, and P. Lastra-Gonzalez, "Tensegrity Applications to Architecture, Engineering and Robotics: A Review", *Applied Sciences*, vol. 13, no. 15, art. no. 8669, 2023, doi: [10.3390/app13158669](https://doi.org/10.3390/app13158669).
- [3] A. Micheletti and P. Podio-Guidugli, "Seventy years of tensegrities (and counting)", *Archive of Applied Mechanics*, vol. 92, no. 9, pp. 2525–2548, 2022, doi: [10.1007/s00419-022-02192-4](https://doi.org/10.1007/s00419-022-02192-4).
- [4] E. Hearney and K. Snelson, *Kenneth Snelson – Art and ideas*. New York: Marlborough Gallery.
- [5] R.B. Fuller, "Tensile-integrity structures", U.S. Patent 3 063 521, Nov. 13, 1962.
- [6] D.G. Emmerich, "Construction de reseaux autotendants", France. Brevet D'invention 1 377 290, 1963.
- [7] K. Snelson, "Continuous tension, discontinuous compression structures", U.S. Patent 3 169 611, Feb. 16, 1965.
- [8] R.E. Skelton and M.C. de Oliveira, *Tensegrity Systems*. New York: Springer, 2009.
- [9] R. Motro, *Tensegrity. Structural Systems for the Future*. London: Kogan Page Science, 2009.
- [10] A. Pugh, *An introduction to Tensegrity*. Berkeley, USA: University of California Press, 1976.
- [11] L.A. Hinrichs, "Prismatic Tensigrids", *Structural Topology*, vol. 9, 1984.
- [12] R. Connelly and M. Terrell, "Globally Rigid Symmetric Tensegrities", *Structural Topology*, vol. 21, 1995.
- [13] J.Y. Zhang, S.D. Guest, and M. Ohsaki, "Symmetric prismatic tensegrity structures: Part I. Configuration and stability", *International Journal of Solids and Structures*, vol. 46, no. 1, pp. 1-14, 2009, doi: [10.1016/j.ijsolstr.2008.08.032](https://doi.org/10.1016/j.ijsolstr.2008.08.032).
- [14] L.Y. Zhang, S.X. Li, S.X. Zhu, B.Y. Zhang, and G.K. Xu, "Automatically assembled large-scale tensegrities by truncated regular polyhedral and prismatic elementary cells", *Composite Structures*, vol. 184, pp. 30–40, 2018, doi: [10.1016/j.compstruct.2017.09.074](https://doi.org/10.1016/j.compstruct.2017.09.074).
- [15] L. Wu and J. Cai, "Generalized prismatic tensegrity derived by dihedral symmetric lines", *International Journal of Solids and Structures*, vol. 305, art. no. 113068, 2024, doi: [10.1016/j.ijsolstr.2024.113068](https://doi.org/10.1016/j.ijsolstr.2024.113068).
- [16] V.A.S.M. Paiva, P.R.G. Kurka, and J.H. Izuka, "Analytical definitions of connectivity, incidence and node matrices for t-struts tensegrity prisms", *Mechanics Research Communications*, vol. 137, art. no. 104271, 2024, doi: [10.1016/j.mechrescom.2024.104271](https://doi.org/10.1016/j.mechrescom.2024.104271).
- [17] Y. Tang, Q. Lv, T. Li, and M. Shao, "Self-equilibrium, stability, and accuracy degradation of imperfect prismatic tensegrities with additional cable nets", *Engineering Structures*, vol. 284, art. no. 115981, 2023, doi: [10.1016/j.engstruct.2023.115981](https://doi.org/10.1016/j.engstruct.2023.115981).
- [18] X. Wang, Z. Zhang, H. Liu, Z. Wang, and M. Zhang, "Morphogenesis analysis of icosahedral and prismatic tensegrity modules", *Thin-Walled Structures*, vol. 205, Part B, art. no. 112500, 2024, doi: [10.1016/j.tws.2024.112500](https://doi.org/10.1016/j.tws.2024.112500).

- [19] A. Al Sabouni-Zawadzka, W. Gilewski, R.N. Charandabi, and A. Zawadzki, "Stability of tensegrity-inspired structures fabricated through additive manufacturing", *Composite Structures*, vol. 345, art. no. 118377, 2024, doi: [10.1016/j.compstruct.2024.118377](https://doi.org/10.1016/j.compstruct.2024.118377).
- [20] A. Al Sabouni-Zawadzka, W. Gilewski, and A. Zawadzki, "Experimental investigations on mechanical properties of 3D-printed tensegrity-inspired metamaterials based on 4-strut simplex module", *Archives of Civil Engineering*, vol. 70, no. 3, pp. 343–357, 2024, doi: [10.24425/ace.2024.150987](https://doi.org/10.24425/ace.2024.150987).
- [21] P. Obara and J. Tomasiak, "Dynamic Stability of Tensegrity Structures – Part II: The Periodic External Load", *Materials*, vol. 16, no. 13, art. no. 4564, 2023, doi: [10.3390/ma16134564](https://doi.org/10.3390/ma16134564).
- [22] P. Obara and J. Tomasiak, "Dynamic Stability of Tensegrity Structures – Part I: The Time-Independent External Load", *Materials*, vol. 16, no. 2, art. no. 580, 2023, doi: [10.3390/ma16020580](https://doi.org/10.3390/ma16020580).
- [23] J. Tomasiak and P. Obara, "The application of the immanent tensegrity properties to control the behavior of double-layered grids", *Archives of Civil Engineering*, vol. 69, no. 1, pp. 131–145, 2023, doi: [10.24425/ace.2023.144164](https://doi.org/10.24425/ace.2023.144164).
- [24] J. Cai, R. Yang, X. Wang, and J. Feng, "Effect of initial imperfections of struts on the mechanical behavior of tensegrity structures", *Composite Structures*, vol. 207, pp. 871–876, 2019, doi: [10.1016/j.compstruct.2018.09.018](https://doi.org/10.1016/j.compstruct.2018.09.018).
- [25] A. Amendola, A. Krushynska, C. Daraio, N.M. Pugno, and F. Fraternali, "Tuning frequency band gaps of tensegrity mass-spring chains with local and global prestress", *International Journal of Solids and Structures*, vol. 155, pp. 47–56, 2018, doi: [10.1016/j.ijsolstr.2018.07.002](https://doi.org/10.1016/j.ijsolstr.2018.07.002).
- [26] Y. Ma, et al., "Meta-tensegrity: Design of a tensegrity prism with metal rubber", *Composite Structures*, vol. 206, pp. 644–657, 2018, doi: [10.1016/j.compstruct.2018.08.067](https://doi.org/10.1016/j.compstruct.2018.08.067).
- [27] L. Małyżko and A. Rutkiewicz, "Response of a tensegrity simplex in experimental tests of a modal hammer at different self-stress levels", *Applied Sciences*, vol. 10, no. 23, art. no. 8733, 2020, doi: [10.3390/app10238733](https://doi.org/10.3390/app10238733).
- [28] A. Rutkiewicz, "Tensegrity Simplex column analysis with different support conditions", *Engineering Structures*, vol. 317, art. no. 118655, 2024, doi: [10.1016/j.engstruct.2024.118655](https://doi.org/10.1016/j.engstruct.2024.118655).
- [29] P. Obara and J. Tomasiak, "Influence of the support conditions on dynamic response of tensegrity grids build with Quartex modules", *Archives of Civil Engineering*, vol. 69, no. 3, pp. 629–644, 2023, doi: [10.24425/ace.2023.146102](https://doi.org/10.24425/ace.2023.146102).
- [30] P. Zhang, K. Kawaguchi, and J. Feng, "Prismatic tensegrity structures with additional cables: Integral symmetric states of self-stress and cable-controlled reconfiguration procedure", *International Journal of Solids and Structures*, vol. 51, no. 25-26, pp. 4294–4306, 2014, doi: [10.1016/j.ijsolstr.2014.08.014](https://doi.org/10.1016/j.ijsolstr.2014.08.014).
- [31] C. Sultan, M. Corless, and R.E. Skelton, "Symmetrical reconfiguration of tensegrity structures", *International Journal of Solids and Structures*, vol. 39, no. 8, pp. 2215–2234, 2002, doi: [10.1016/S0020-7683\(02\)00100-2](https://doi.org/10.1016/S0020-7683(02)00100-2).
- [32] K. Kawaguchi and S. Ohya, "Monitoring of full-scale tensegrity skeletons under temperature change", in *Symposium of the International Association for Shell and Spatial Structures: Evolution and Trends in Design, Analysis and Construction of Shell and Spatial Structures: Proceedings, IASS Symposium 2009, 28 September – 2 October 2009, Valencia, Spain*, A. Domingo Cabo, et al., Eds. València: Editorial Universitat Politècnica de València, 2009, pp. 224–231.
- [33] K. Kawaguchi, S. Ohya, and S. Vormus, "Long-Term Monitoring of White Rhino, Building with Tensegrity Skeletons", presented at The 35th Annual Symposium of IABSE / 52nd Annual Symposium of IASS / 6th International Conference on Space Structures: Taller, Longer, Lighter - Meeting growing demand with limited resources, September 2011, London, United Kingdom, 2011.
- [34] M. Eekbout, "Architecture in space structures", PhD thesis, University of Delft, the Netherlands, 1989.
- [35] A. Rutkiewicz and L. Małyżko, "Eigenmode analysis at self-stress state of a quartex tensegrity tower", in *Lightweight Structures in Civil Engineering XXV*, P. Bilko and L. Małyżko, Ed. Olsztyn: University of Warmia and Mazury Press, 2019, pp. 38–39.
- [36] Y. Tang, Q. Lv, T. Li, and M. Shao, "Self-equilibrium, stability, and accuracy degradation of imperfect prismatic tensegrities with additional cable nets", *Engineering Structures*, vol. 284, art. no. 115981, 2023, doi: [10.1016/j.engstruct.2023.115981](https://doi.org/10.1016/j.engstruct.2023.115981).
- [37] J. Feron and P. Latteur, "Implementation and propagation of prestress forces in pin-jointed and tensegrity structures", *Engineering Structures*, vol. 289, art. no. 116152, 2023, doi: [10.1016/j.engstruct.2023.116152](https://doi.org/10.1016/j.engstruct.2023.116152).
- [38] F. Fraternali, G. Carpenteri, and A. Amendola, "On the mechanical modeling of the extreme softening/stiffening response of axially loaded tensegrity prisms", *Journal of the Mechanics and Physics of Solids*, vol. 74, pp. 136–157, 2015, doi: [10.1016/j.jmps.2014.10.010](https://doi.org/10.1016/j.jmps.2014.10.010).

- [39] L. Zhang and G. Xu, "Negative stiffness behaviors emerging in elastic instabilities of prismatic tensegrities under torsional loading", *International Journal of Mechanical Sciences*, vol. 103, pp. 189–198, 2015, doi: [10.1016/j.ijmecsci.2015.09.009](https://doi.org/10.1016/j.ijmecsci.2015.09.009).
- [40] P. Obara, J. Kłosowska, and W. Gilewski, „Truth and Myths about 2D Tensegrity Trusses”, *Applied Sciences*, vol. 9, no. 1, art. no. 179, 2019, doi: [10.3390/app9010179](https://doi.org/10.3390/app9010179).
- [41] I. Wójcik-Grząba, "Form-finding of optimal cable nets under self-weight based on the Force Density Method", *Archives of Civil Engineering*, vol. 70, no. 3, pp. 241–256, 2024, doi: [10.24425/ace.2024.150981](https://doi.org/10.24425/ace.2024.150981).
- [42] S. Carstens and D. Kuhl, "Non-linear static and dynamic analysis of tensegrity structures by spatial and temporal Galerkin methods", *Journal of the International Association for Shell and Spatial Structures*, vol. 46, no. 148, pp. 116–134, 2005.

Sprężanie nieminimalnego modułu tensegrity triplex

Słowa kluczowe: kratownica, moduł nieminimalny, równania energii, sprężenie wstępne, tensegrity triplex

Streszczenie:

W artykule przedstawiono przykłady analiz stabilnych konfiguracji sprężonych modułów tensegrity triplex o nieminimalnej liczbie elementów. Nieminimalny triplex jest prezentowany obecnie w literaturze jako wersja minimalna z trzema dodatkowymi cięgnami. Przeprowadzone analizy pokazują jednak, że podczas sprężania można uzyskać wiele różnych konfiguracji modułu, nie zaś tylko jedną. Procedura sprężania prowadzona jest poprzez zmianę długości wybranych grup elementów, tj. zastrzałów, cięgien poziomych, cięgien ukośnych lub dodatkowych elementów, przy założeniu symetrii. Ponadto, przedstawiono alternatywne podejście do sprężania o przejrzystej interpretacji fizycznej. Równania zapisane są w formie analitycznej za pomocą podejścia energetycznego, zaś rozwiązywane są numerycznie. W pracy przedstawiono dwa przykłady sprężania nieminimalnych modułów triplex - smukłego i krępego. Wyniki pokazują, że dodatkowe elementy, w literaturze zawsze traktowane jako cięgna, mogą również służyć jako zastrzały, co prowadzi do powstania nowej grupy konstrukcji o cechach tensegrity.

Received: 2025-02-20, Revised: 2025-03-04